THERMOELECTRIC SELF-COOLING FOR POWER ELECTRONICS: INCREASING THE COOLING POWER

Alvaro Martinez*, David Astrain, Patricia Aranguren

Mechanical, Energy and Materials Engineering Department

Public University of Navarre, 31006 Pamplona, Spain

Smart Cities Institute, 31006 Pamplona, Spain

Tel: +34 948 169309, Fax: +34 948 169099, e-mail: alvaro.martinez@unavarra.es

Abstract

Thermoelectric self-cooling was firstly conceived to increase, without electricity consumption, the cooling power of passive cooling systems. This paper studies the combination of heat pipe exchangers and thermoelectric self-cooling, and demonstrates its applicability to the cooling of power electronics.

Experimental tests indicate that source-to-ambient thermal resistance reduces by around 30 % when thermoelectric self-cooling system is installed, compared to that of the heat pipe exchanger under natural convection. Neither additional electric power nor cooling fluids are required. This thermal resistance reaches 0.346 K/W for a heat flux of 24.1 kW/m^2, being one order of magnitude lower than that obtained in previous designs. In addition, the system adapts to the cooling demand, reducing this thermal resistance for increasing heat.

Simulation tests have indicated that simple system modifications allow relevant improvements in the cooling power. Replacement of a thermoelectric module with a thermal bridge leads to 33.54 kW/m^2 of top cooling power. Likewise, thermoelectric modules with shorter legs and higher number of pairs lead to a top cooling power of 44.17 kW/m^2. These results demonstrate the applicability of thermoelectric self-cooling to power electronics.

Keywords: thermoelectric self-cooling; power electronics; Seebeck effect; heat pipe exchanger

NOMENCLATURE

b	Systematic standard uncertainty	
I	Electric current	A
k	Thermal conductivity of the thermal bridge	W/mºC
L	Leg length	mm
N	Number of thermoelectric pairs in a thermoelectric module	
P	Electric power supplied by the modules to the fan	W
$\dot{Q}$	Heat flux generated by the heat source	W
R	Thermal resistance	ºC/W
T	Temperature	ºC
V	Electric voltage	V
ΔT	Source-to-ambient temperature difference	ºC

Subscripts

amb	Ambient
c	Convective heat transfer
eq	Equivalent of thermoelectric modules and thermal bridge
hp	Heat pipe exchanger
mod	Thermoelectric module
source	Heat source

1- INTRODUCTION

Cooling and thermal management of electronic devices is a growing challenge in the field of power electronics, from small microprocessors to large electric power converters. It is a fact, that recent developments always involve higher electric power and smaller size, which inevitably leads to higher cooling demands.

Anandan [1] categorized thermal management systems into active and passive, those in the former being able to provide higher cooling power than those in the latter, but also requiring electric power for operation. Forced air/liquid convection, air/liquid jet impingement and refrigeration systems belong to this group.

However, as this author underlines, when electric power consumption and/or space limitation are key issues, passive techniques are more practical. Effective heat spreaders attached to finned heat sinks are the most used passive cooling techniques. Nowadays, heat pipe exchangers are under deep investigation. As indicated by Jouhara [2] and Chernysheva [3], a heat pipe exchanger presents continuous vaporization and condensation of an enclosed fluid, which leads to extremely high heat transfer coefficients. Furthermore, no electric power is needed to pump the fluid. Onn the other hand, working as a passive cooling system (i.e. under natural convection) a heat pipe exchanger presents limited cooling power.

In this regard, thermoelectric self-cooling (TSC) sets out to increase the cooling power of passive cooling systems. Contrary to other techniques, this technology increases the cooling power without additional electric power consumption. As Martinez indicates [4], this technology transforms a passive cooling system into an active cooling system, but requires no electric power to perform this process. The basic layout of a TSC includes several thermoelectric modules installed between a heat source and a passive cooling system. By Seebeck effect, the modules transform part of the heat emitted by the source into electricity, which is directly used to operate a fan installed over the passive system. As a consequence, the cooling power increases without electric power consumption.

This concept was firstly proposed by Yazawa [5], who applied it to the cooling of a 11.6x11.6 mm^2 microprocessor. Yazawa's prototype included one "off-the-shelf" thermoelectric module operating a fan installed over a finned heat sink. This author reported source-to-ambient (or global) thermal resistances of around 4 K/W, which despite far from being acceptable for microprocessor cooling, resulted 40 % lower than the thermal resistance provided by an optimized passive cooling system under similar working conditions. Note that the comparison was valid, since none of the systems consumed electric power. Yazawa's work showed the potential of TSC and established lines for improvement, which involved the reduction of the high thermal resistance of the heat sink.

The first improvement for microprocessor cooling was provided by Solbrekken [6], who introduced a secondary path for the heat flux. Thus, only a part of the heat crossed the module and the finned heat sink, whereas the rest went through another finned heat sink. As a result, Solbrekken was able to halve the global thermal resistance to 2 K/W. Furthermore, he stated that a thermal resistance of around 1 K/W for 50ºC of source-to-ambient temperature difference would be required for reliable microprocessor cooling.

One step further, Kiflemariam confirmed that the thermal resistance of the heat sink acts as bottleneck [7], so he replaced it with a complete microfluidic dissipation system, composed of a microchannel heat sink, fluid conduits, a secondary heat sink and a pump [8]. For a 15x15 mm^2 heat source, this author reported global thermal resistance of around 1.3 K/W, almost independent of source-to-ambient temperature difference. The idea of introducing fluidic heat sinks is correct in terms of heat transfer, since higher convection coefficients are achievable, as this author indicates. However, loss of compactness is obvious, compared to previous designs, thus limiting its applicability. Furthermore, the electric power consumption increases, since the modules not only must provide force convection to the secondary heat sink but also operate the driving pump.

Martinez applied Yazawas's TSC to power electronics [4], where the number of potential applications seems enormous. Electric power converters, transformers, control systems, etc. present cooling demands of at least 25 kW/m^2 but low working temperatures, so that source-to-ambient temperature difference is usually limited to 80 ºC, as stated by Buttay [9] and Anandan [1]. Martinez developed a prototype for a 220x160 mm^2 heat source, which included 4 thermoelectric modules that operated a fan installed over a finned heat sink. For the cited source-to-ambient temperature difference, 140 W of dissipated heat was obtained, leading to 0.57 K/W of global thermal resistance, 30 % lower than that provided by the finned heat sink working under natural convection. The cooling power reached 4 kW/m^2, far from 25 kW/m^2 required by low-power electronic devices. Again, the thermal resistance of the heat sink was too high, accounting for around 40 % of the global thermal resistance. This author also developed a computational model for TSC applications [10], and demonstrated that this first design could be directly applied to prevent overheating in solar collectors, obtaining a low-power-consumption [11] or even zero-power-consumption [12] thermal management system.

The present paper goes one step further, aiming to increase the cooling power of TSC to surpass 25 kW/m^2, so that these systems could be used in the cooling of power electronics. To do so, the combination of heat pipe exchangers and TSC is evaluated.

The paper presents two primary objectives: The first one is to compare the heat removed from a hot spot by a heat pipe exchanger under natural convection, and that removed by a TSC that uses a similar heat pipe. The objective is to show the potential of TSC and prove that the cooling power of a heat pipe could be increased without electric power consumption. To this end, section 2 describes the TSC test bench, presenting the arrangement of the heat source, the heat pipe exchanger and the thermoelectric modules; section 3 describes the methodology used in this experimental study; and, finally, section 4.1 presents the results.

The second objective is to increase the cooling power of the TSC used in the previous experimental study. Two approaches are proposed, and the performance is assessed by a simulation process that involves the use of a computational model developed specifically for TSC applications [10]. Results are presented in section 4.2. Finally, section 5 provides the main conclusions of the paper.

2- TEST BENCH DESCRIPTION

2.1- Heat source

As can be seen in Figs. 1 & 2, the heat source consists of a 120x80x10 mm^3 aluminium block containing five cartridge heaters, connected electrically in parallel to an adjustable Grelco GVD electric power supply [13]. It has been considered that 100 % of the electric power produced by this Grelco GVD is transformed into heat power.

Furthermore, this power supply presents 4 Ω of internal electric resistance –that is, voltage is always four times higher than electric current.

2.2- Heat pipe exchanger

The heat exchanger is composed of 10 heat pipes, 350 mm long and 8 mm of diameter, containing depressurized water. A 140x100x12 mm^3 aluminium block is installed at the hot side of the pipes, whereas 56 aluminium fins, each one with 130x57x0.5 mm^3 and separated 3 mm, are included to increase the heat transfer surface area from the cold side of the pipes to the ambient. Figure 1 shows this configuration (wherein the heat source is slightly displaced for clarification). All free surfaces (that is, top surface of the heat source and bottom surface of the block) are thoroughly insulated with rockwool layers.

2.3- TSC experimental setup

The TSC includes the cited heat pipe exchanger and 6 Marlow TG12-8 thermoelectric modules [14], connected electrically in series. Each module presents 40x40x3.5 mm^3 and is able to work up to 200 ºC in continuous operation. Figure 2 shows the assembly of the modules, the heat pipe exchanger and the heat source. The heat source is totally covered by the modules. Again, all free surfaces are insulated with rockwool layers.

A wind tunnel and a Sunon-KD1212PTB1 [15] axial fan, with 5.2 W of electric power consumption at 12 V, are installed over the fins to provide force convection. As already stated, the thermoelectric modules supply the power required by the fan. In this respect, Martinez [4] indicated that the electric power generated by the modules is maximum when being connected to a load equal to their internal electrical resistance or a bit higher. That of six Marlow TG12-8 in series reaches around 20 Ω, close to the 27 Ω presented by the fan.

Finally, Ahlborn T190-0 NiCr-Ni thermo-wires [16] are used as temperature sensors, connected to an Ahlborn Almemo 5690-1M09 data acquisition system [17]. Two of them are used to calculate the source temperature, other two for that at the top surface of the modules, six spread along the fins, and two measure the ambient temperature. The electric power generated by the modules (and consumed by the fan) is directly measured with a multimeter Gossen Metrawatt Metra Hit 29S [18].

3- METHODOLOGY

The parameter used to evaluate the thermal performance of the system is the cited source-to-ambient thermal resistance (or global thermal resistance), provided by Eq. (1). Given the aforementioned insulation, no heat losses are considered (that is, heat is transferred directly from the heat source to the ambient).

$$R = \frac{T_{\text{source}} - T_{\text{amb}}}{\dot{Q}} = \frac{T_{\text{source}} - T_{\text{amb}}}{V_{\text{source}} I_{\text{source}}} = \frac{T_{\text{source}} - T_{\text{amb}}}{V_{\text{source}}^2 / 4} \tag{1}$$

This experimental work aims to obtain and compare the global thermal resistance for two configurations. For configuration 1, the heat pipe exchanger working under natural convection is attached to the heat source. As can be seen in the electrical analogy presented in Fig. 1, the global thermal resistance is the sum of the thermal resistance of the heat pipe exchanger and the pipes-to-ambient convective thermal resistance.

For configuration 2, a TSC system is attached to the heat source, as Fig. 2 shows. In this configuration, the global thermal resistance comprises also the equivalent thermal resistance of six modules in parallel. Additionally, one could have in mind another thermal path that has not been considered in the study, namely, the heat transferred to the ambient from the external surface of the tubes that is not covered neither by thermal insulation nor by the wind tunnel. This thermal path is negligible given that, firstly, the external surface of the tubes is almost two orders of magnitude lower than that of the fins; and, secondly, the convective heat transfer coefficient in the tubes (natural convection) is at least one order of magnitude lower than that in the fins (forced convection).

These electrical analogies are simplistic system representations; they are not intended to simulate the real system performance, but to roughly show which component (which thermal resistance) is the bottleneck of the application and should be addressed to increase the cooling power.

The uncertainty analysis is based on Coleman's works [19]. Thus, every output is provided along with its overall uncertainty to form the corresponding 95% confidence interval. The overall uncertainty is composed of the random standard uncertainty for the mean (three runs of every experiment are conducted) and the systematic standard uncertainty. Table 1 provides the systematic standard uncertainty for all the measured parameters, whereas those for the outputs are calculated with Eqs. (2)-(6).

$$b_{\dot{\mathrm{Q}}}^2 = I_{\mathrm{source}}^2 b_{\mathrm{Vsource}}^2 + V_{\mathrm{source}}^2 b_{\mathrm{Isource}}^2 = \left(\frac{\dot{Q}}{V_{\mathrm{source}}}\right)^2 b_{\mathrm{Vsource}}^2 + \left(\frac{4\dot{Q}}{V_{\mathrm{source}}}\right)^2 b_{\mathrm{Isource}}^2 \qquad (2)$$

$$b_{\mathrm{R}}^2 = \left(\frac{1}{I_{\mathrm{source}} V_{\mathrm{source}}}\right)^2 b_{\mathrm{T}}^2 + \left(\frac{T_{\mathrm{source}} - T_{\mathrm{amb}}}{I_{\mathrm{source}}^2 V_{\mathrm{source}}^2}\right)^2 b_{\dot{\mathrm{Q}}}^2 = \left(\frac{1}{\dot{Q}}\right)^2 b_{\mathrm{T}}^2 + \left(\frac{R}{\dot{Q}}\right)^2 b_{\dot{\mathrm{Q}}}^2 \qquad (3)$$

$$b_{\mathrm{Rmod}}^2 = \left(\frac{1}{I_{\mathrm{source}}V_{\mathrm{source}}}\right)^2 b_{\mathrm{T}}^2 + \left(\frac{T_{\mathrm{source}} - T_{\mathrm{mod}}}{I_{\mathrm{source}}^2 V_{\mathrm{source}}^2}\right)^2 b_{\dot{\mathrm{Q}}}^2 = \left(\frac{1}{\dot{Q}}\right)^2 b_{\mathrm{T}}^2 + \left(\frac{R_{\mathrm{mod}}}{\dot{Q}}\right)^2 b_{\dot{\mathrm{Q}}}^2 \qquad (4)$$

$$b_{\mathrm{Rhp}}^2 = \frac{5}{3}\left(\frac{1}{I_{\mathrm{source}}V_{\mathrm{source}}}\right)^2 b_{\mathrm{T}}^2 + \left(\frac{T_{\mathrm{mod}} - T_{\mathrm{hp}}}{I_{\mathrm{source}}^2 V_{\mathrm{source}}^2}\right)^2 b_{\dot{\mathrm{Q}}}^2 = \frac{5}{3}\left(\frac{1}{\dot{Q}}\right)^2 b_{\mathrm{T}}^2 + \left(\frac{R_{\mathrm{hp}}}{\dot{Q}}\right)^2 b_{\dot{\mathrm{Q}}}^2 \qquad (5)$$

$$b_{\mathrm{Rc}}^2 = \frac{2}{3}\left(\frac{1}{I_{\mathrm{source}}V_{\mathrm{source}}}\right)^2 b_{\mathrm{T}}^2 + \left(\frac{T_{\mathrm{hp}} - T_{\mathrm{amb}}}{I_{\mathrm{source}}^2 V_{\mathrm{source}}^2}\right)^2 b_{\dot{\mathrm{Q}}}^2 = \frac{2}{3}\left(\frac{1}{\dot{Q}}\right)^2 b_{\mathrm{T}}^2 + \left(\frac{R_{\mathrm{c}}}{\dot{Q}}\right)^2 b_{\dot{\mathrm{Q}}}^2 \qquad (6)$$

4- RESULTS AND DISCUSSION

4.1- Experimental study: TSC versus heat pipe exchanger under natural convection

The prototype is installed inside a climatic chamber to fix the ambient temperature and humidity at 20 ºC and 50 % respectively. For different generated heat, all thermal resistances are calculated, along with the electric power provided by the modules to the fan in configuration 2. As indicated in section 1, the maximum permitted source-to-ambient temperature difference is set at 80 ºC. The test is replicated twice and the results presented in Tables 2 and 3.

With respect to configuration 1 (heat pipe exchanger under natural convection), the convective thermal resistance accounts for around 90 % of the global thermal resistance in all scenarios. As expected, this thermal resistance reduces for increasing heat, since increasing pipes-to-ambient temperature difference occurs, which enhances heat transfer by natural convection. This effect, along with the virtually constant thermal resistance of the heat pipe exchanger, explains the inverse relation between the global thermal resistance and the heat flux.

As for configuration 2, global thermal resistances are significantly lower than those of configuration 1, which means that the decrease in this thermal resistance caused by the forced convection outweighs the increase caused by the addition of thermoelectric modules in the path of the heat flux. For increasing heat, temperature difference in the modules increases and so does the electric power supplied to the fan [4]. As a consequence, the forced convection is enhanced so that both the convective and the global thermal resistance reduce. In other words, the TSC system adapts to the cooling demand, reducing the global resistance for increasing heat.

As expected, the thermal resistance of the heat pipe exchanger remains virtually constant and similar to that obtained for configuration 1. As for the modules, the manufacturer indicates a thermal resistance between 1.2 and 1.3 K/W for a single module in the used temperature range [14], which results in 0.20-0.22 K/W for six modules in parallel, thus confirming the results.

Figure 3 shows the global thermal resistance versus the source-to-ambient temperature difference for both configurations. As can be seen, this thermal resistance reduces by around 30 % in all scenarios when TSC is used. The minimal thermal resistance occurs for 80 ºC, reaching 0.346 K/W. For this source-to-ambient temperature difference, the TSC system is able to dissipate 231 W (24,1 kW/m^2), whereas the heat pipe exchanger under natural convection reaches 149 W (15,5 kW/m^2), with 0.537 of global thermal resistance. For the latter to reach 24,1 kW/m^2 a 55% of additional convective surface area would be required. This fact shows the gain in compactness that entails the use of TSC systems. With 24,1 kW/m^2, this TSC design stays at the borderline of being applicable for the cooling of power electronics.

Noteworthy is also the reduced improvement in the global thermal resistance that occurs in configuration 2 for increased heat, even though the modules provide four-times-higher electric power to the fan (from 1.1 to 4.4 W). The reason can be seen in Fig. 4, which shows the individual thermal resistances of the TSC components. The thermal resistance of the thermoelectric modules acts as bottleneck of this application, accounting for around 60 % of the global thermal resistance, whereas that of the heat pipe exchanger account for around 25 %. As a consequence, any improvement in the convective thermal resistance has little impact on the global thermal resistance.

In conclusion, this experimental study provides two relevant aspects. Firstly, the modules generate more electric power than required, since no significant increase in cooling power occurs for higher values. Secondly, a decrease in the thermal resistance of the thermoelectric modules would lead to a decrease in the global thermal resistance and, in turn, to higher cooling power. The combination of these two aspects indicates that the best approach for reducing the global thermal resistance (or equivalently, for increasing the cooling power) is to reduce the thermal resistance of the thermoelectric modules. This measure would inevitably reduce the electric power to the fan, thus increasing the convective thermal resistance. Therefore, the exact balance between these opposing facts must be found. Section 4.2 present two measures to apply this approach.

4.2- Increasing the cooling power of the TSC

The first measure involves the modification of the module architecture. Thus, several values of leg length and number of thermoelectric pairs are evaluated to assess their influence on the global thermal resistance and cooling power. It is clear that either an increase in the number of legs or a reduction in the leg length would lead to a reduction in the module thermal resistance.

The second one involves the use of thermal bridges in parallel with the thermoelectric modules, so that two heat paths emerge. The low thermal resistance of the bridge would make the equivalent thermal resistance significantly lower than that of the modules.

A computational model for TSC applications is used to evaluate these two measures [10]. The model predicts voltage, electric current and electric power generated by the modules, global efficiency, temperatures and heat fluxes. The model is deterministic, therefore no randomness is included in the inputs.

For steady-state simulation, the model requires module dimensions (legs and ceramic layers); total number of modules and pairs; temperature-dependent thermoelectric properties of n-doped and p-doped legs (thermal conductivity, Seebeck coefficient, electrical resistivity and surface electrical resistivity); heat flux produced by the source; ambient temperature; electric load resistance of the fan; thermal resistance of the heat pipe exchanger; and pipe-to-ambient thermal resistance as a function of the electric power provided by the modules to the fan.

Table 4 presents the values of all these inputs, taken from Martinez's works [10], [20]. Number of modules, number of pairs, and leg length vary along simulations.

4.2.1- Improvement #1: Module architecture

For all simulations, source-to ambient temperature difference is set at 80ºC. The number of thermoelectric pairs is set at 127 or 254, typical of "off-the-shelf" modules. Leg length is reduced from 1.3 mm (Marlow TG12-8) to 0.2 mm. The model provides the cooling power under these conditions, along with all the thermal resistances, electric power and voltage supplied by the modules to the fan. Table 5 shows the results.

It can be seen that the thermal resistance of the modules decrease as length reduces, which also leads to lower electric power to the fan, and in turn to increasing values of convective thermal resistance. However, the decrease in the module resistance outweighs the increase in the convective resistance, so that the final effect is a decrease in the global resistance and an increase in the cooling power. Once the maximum is reached, the dissipated heat reduces since now the latter outweighs the former. Maximum cooling power occurs at 0.3 mm for 127 pairs, and 0.4 mm. for 254 pairs, reaching 364 W (37.92 kW/m^2) and 424 W (44.17 kW/m^2) respectively.

4.2.2- Improvement #2: Thermal bridge

This measure involves the substitution of thermoelectric modules by thermal bridges equal in size, in order to reduce the source-to-pipe thermal resistance. Compared to the previous measure, the main advantage lays in the reduction of cost, since a lower number of thermoelectric modules is used. This experiment proposes the removal of one or two thermoelectric modules, which are replaced with thermal bridges with increasing thermal conductivity. The thermal resistance of the bridge is composed of the conductive thermal resistance, plus a contact resistance at either side with 15625 W/m^{2}K of heat transfer coefficient, typical of metal interfaces covered with conductive paste, as Astrain indicates [21] . Again, source-to ambient temperature difference is set at 80ºC. Table 6 shows the results.

First row presents the original case, in which six modules are used, so no thermal bridge is needed. Then, one module is replaced with a thermal bridge with increasing conductivity. The equivalent thermal resistance reduces, which decreases the temperature difference between ends of the modules and the electric power supplied to the fan. As a result, the convective thermal resistance increases. The former fact outweighs the latter, so the global thermal resistance decreases, thus increasing the cooling power. This effect holds until a maximum of 322 W (33.54 kW/m^2) is reached, at 100 W/mK of thermal conductivity.

Similar explanations apply to the second case, when two modules are removed. In this case, the maximum dissipated heat is 297 W (30.94 kW/m^2) and occurs at 25 W/mK of thermal conductivity. The rapid decrease in the electric power supplied to the fan constrains the effectivity of this case.

5- CONCLUSIONS

Thermoelectric self-cooling systems were firstly conceived to increase the cooling power of passive cooling systems. Thermoelectric modules transform part of the heat emitted by a heat source into electricity, which is directly used to operate a fan installed over the passive system. As a consequence, the cooling system becomes active, thus increasing the cooling power without external electric power consumption.

The cooling power of these systems has been growing since the first design came out, by moving from finned heat sinks to fluidic systems. Now, this paper has studied the combination of heat pipe exchangers and thermoelectric self-cooling, and assessed its applicability to the cooling of power electronics.

Experimental results have indicated that source-to-ambient thermal resistance reduces by around 30 % when thermoelectric self-cooling system is installed, compared to that of the heat pipe exchanger under natural convection. For 80 ºC of source-to ambient temperature difference, cooling power of 231 and 149 W have been obtained respectively. For the latter to reach 231 W, fin surface should be increased by 55%, which shows the gain in compactness that entails the use of thermoelectric self-cooling. Furthermore, the system adapts to the cooling demand, reducing the global resistance for increasing heat.

With 24.1 kW/m^2, this first design stays at the borderline of being applicable for the cooling of power electronics. Furthermore, simulation tests have indicated that simple system modifications, aiming to reduce the thermal resistance of the modules, allow relevant improvement in the cooling power. In the first place, thermoelectric modules with shorter legs and higher number of pairs have been used. A top cooling power of 44.17 kW/m^2 was obtained for six modules with 254 pairs, 0.4 mm long. Secondly, thermal bridges were installed replacing one or two thermoelectric modules. In this case, a top cooling power of 33.54 kW/m^2 has been obtained for five original modules and a thermal bridge with 100 W/mK of thermal conductivity.

Despite the fact that this paper is focused on heat dissipation from power electronic devices, it is clear that the number of potential applications of thermoelectric self-cooling is huge in the field of micro/mini electronics. In this regard, scalability is certainly one of the main characteristics of thermoelectric devices, so that not only thin film but also micro-modules could be applied. This fact combines to recent developments in heat pipe miniaturization to allow practical applications of thermoelectric self-cooling to the heat dissipation from hot devices a few millimeters in size. In theory, every application that uses a passive heat pipe for cooling purposes – either micro, mini or normal size- would benefit from the inclusion of this technology, as it increases the cooling power and requires only extra space for one or several thermoelectric modules and a fan.

All these comments allow stating that thermoelectric self-cooling systems present good prospects for the cooling of power electronics, from microprocessors to bigger devices.

ACKNOWLEDGMENTS

The authors would like to thank the Spanish Ministry of Economy and Competitiveness (DPI2014-53158-R) and FEDER Funds (European Union) for supporting this work.

REFERENCES

[1] S. Anandan and V. Ramalingam, “Thermal management of electronics: A review of literature,” *Therm. Sci.*, vol. 12, no. 2, pp. 5–25, 2008.

[2] H. Jouhara, Z. Ajji, Y. Koudsi, H. Ezzuddin, and N. Mousa, “Experimental investigation of an inclined-condenser wickless heat pipe charged with water and an ethanol-water azeotropic mixture,” *Energy*, vol. 61, pp. 139–147, 2013.

[3] M. Chernysheva, S. Yushakova, and Y. Maydanik, “Copper-water loop heat pipes for energy-efficient cooling systems of supercomputers,” *Energy*, vol. 69, pp. 534–542, 2014.

[4] A. Martínez, D. Astrain, and A. Rodríguez, “Experimental and analytical study on thermoelectric self cooling of devices,” *Energy*, vol. 36, no. 8, pp. 5250–5260, 2011.

[5] K. Yazawa, G. L. Solbrekken, and A. Bar-Cohen, “Thermoelectric-powered convective cooling of microprocessors,” *IEEE Trans. Adv. Packag.*, vol. 28, no. 2, pp. 231–239, 2005.

[6] G. L. Solbrekken, K. Yazawa, and A. Bar-Cohen, “Heat driven cooling of portable electronics using thermoelectric technology,” *IEEE Trans. Adv. Packag.*, vol. 31, no. 2, pp. 429–437, 2008.

[7] R. Kiflemariam and C. Lin, “Numerical Simulation and Parametric Study of Heat-Driven Self-Cooling of Electronic Devices,” *J. Therm. Sci. Eng. Appl.*, vol. 7, no. 1, p. 011008, 2014.

[8] R. Kiflemariam and C. Lin, “Numerical simulation of integrated liquid cooling and thermoelectric generation for self-cooling of electronic devices,” *Int. J. Therm. Sci.*, vol. 94, pp. 193–203, 2015.

[9] C. Buttay, D. Planson, B. Allard, D. Bergogne, P. Bevilacqua, C. Joubert, M. Lazar, C. Martin, H. Morel, D. Tournier, and C. Raynaud, “State of the art of

high temperature power electronics," *Mater. Sci. Eng. B*, vol. 176, no. 4, pp. 283–288, 2011.

[10] A. Martínez, D. Astrain, and A. Rodríguez, "Dynamic model for simulation of thermoelectric self cooling applications," *Energy*, vol. 55, pp. 1114–1126, 2013.

[11] A. Martínez, D. Astrain, A. Rodríguez, and P. Aranguren, "Thermoelectric Self-Cooling System to Protect Solar Collectors from Overheating," *J. Electron. Mater.*, vol. 43, no. 6, pp. 1480–1486, 2013.

[12] A. Martínez, D. Astrain, and A. Rodríguez, "Zero-power-consumption thermoelectric system to prevent overheating in solar collectors," *Appl. Therm. Eng.*, vol. 73, no. 1, pp. 1101–1110, 2014.

[13] "Grelco GVD." [Online]. Available: www.grelco.com/pdfEsp/GVD.pdf.

[14] "Marlow TG12-8." [Online]. Available: http://www.marlow.com/media/marlow/product/downloads/tg12-8-01ls/TG12-8_Data_Sheet_RevM.pdf.

[15] "Sunon KD1212PTB1." [Online]. Available: http://datasheetz.com/data/Fans/DC/KDE1212PTB1-6A-datasheetz.html.

[16] "Ahlborn T190-0." [Online]. Available: www.ahlborn.com/getfile.php?1966.pdf.

[17] "Ahlborn Almemo 5690-1M09." [Online]. Available: http://www.ahlborn.com/getfile.php?1523.pdf.

[18] "Gossen Metrawatt Metra Hit 29S." [Online]. Available: https://www.gossenmetrawatt.com/resources/zz_tam/hit28-29s/db_gb.pdf.

[19] H. Coleman and W. Steele, *Experimentation, Validation, and Uncertainty Analysis for Engineers*, 3rd ed. Hoboken, NJ: John Wiley & Sons, 2009.

[20] A. Martínez, J. Vián, D. Astrain, A. Rodríguez, and I. Berrio, "Optimization of the heat exchangers of a thermoelectric generation system," *J. Electron. Mater.*, vol. 39, no. 9, pp. 1463–1468, 2010.

[21] D. Astrain, A. Martínez, and A. Rodríguez, "Improvement of a thermoelectric and vapour compression hybrid refrigerator," *Appl. Therm. Eng.*, vol. 39, pp. 140–150, 2012.

FIGURE CAPTIONS

Fig. 1. Heat pipe exchanger and heat source. Electrical analogy of configuration 1.

Fig. 2. Thermoelectric self-cooling system. Electrical analogy of configuration 2.

Fig. 3. Global thermal resistances for both configurations versus source-to-ambient temperature difference.

Fig. 4. Thermal resistances for the TSC components.

TABLES

Variable	Device	b
T	Ahlborn T190-0	0.15 ºC
V_{source}	Grelco GVD	0.5 V
I_{source}	Grelco GVD	0.025 A
P	Gossen Metrawatt Metra Hit 29S	0.05 W

Table 1. Systematic standard uncertainties.

$\dot{Q}$ (W)	R (K/W)	R_{hp} (K/W)	R_c (K/W)
49.94±0.84	0.719±0.014	0.102±0.009	0.617±0.011
100.03±1.12	0.591±0.012	0.095±0.006	0.496±0.008
149.98±1.45	0.537±0.006	0.092±0.004	0.444±0.004

Table 2. Experimental results for configuration 1 (heat pipe exchanger under natural convection).

$\dot{Q}$ (W)	R (K/W)	R_{mod} (K/W)	R_{hp} (K/W)	R_c (K/W)	P (W)
109.94±1.48	0.380±0.006	0.217±0.004	0.088±0.004	0.075±0.003	1.1±0.1
150.20±1.39	0.368±0.004	0.218±0.006	0.094±0.005	0.056±0.002	2.0±0.2
189.50±1.54	0.358±0.004	0.217±0.002	0.093±0.003	0.048±0.001	3.1±0.1
229.59±1.73	0.346±0.004	0.217±0.002	0.088±0.003	0.041±0.002	4.4±0.1

Table 3. Experimental results for configuration 2 (TSC).

M	variable	$\alpha_p = -\alpha_n$	$10^{-6}(-0.002025T^{2} + 1.423448T - 44.953611)$ V/K
N	variable	$k_p = k_n$	$0.000029\ T^2 - 0.019593T + 4.809677$ W/mK
L	variable	$\sigma_p = \sigma_n$	$10^{-6}(0.043542T - 2.754139)$ Ωm
S	1.4 x 1.4 mm	σ^s	0.11 Ωm^2
L_{ce}	0.8 mm	R_{hp}	0.091 K/W
S_{ce}	40 x 40 mm	R_{chp}	$0{,}0758\ P^{-0{,}418}$ K/W
Rl	26.6 Ω	T_e	20 ºC

Table 4. Input parameters for simulation.

N	L (mm)	$\dot{Q}$ (W)	R (K/W)	R_{mod} (K/W)	R_{hp} (K/W)	R_c (K/W)	P (W)	V (V)
127	1.30	232	0.344	0.213	0.091	0.040	4.5	11.0
127	1.10	252	0.317	0.186	0.091	0.040	4.4	10.8
127	0.90	276	0.290	0.157	0.091	0.042	4.1	10.4
127	0.70	305	0.262	0.127	0.091	0.044	3.5	9.6
127	0.50	338	0.237	0.096	0.091	0.050	2.6	8.3
127	0.40	354	0.226	0.079	0.091	0.056	2.0	7.3
127	0.30	364	0.220	0.062	0.091	0.067	1.3	5.9
127	0.20	351	0.228	0.043	0.091	0.094	0.6	4.0
254	1.30	350	0.229	0.098	0.091	0.040	4.7	11.2
254	1.10	368	0.217	0.086	0.091	0.040	4.5	10.9
254	0.90	388	0.206	0.073	0.091	0.042	4.1	10.4
254	0.70	408	0.196	0.060	0.091	0.045	3.4	9.5
254	0.60	417	0.192	0.054	0.091	0.047	3.0	8.9
254	0.50	423	0.189	0.047	0.091	0.052	2.5	8.2

254	0.40	424	0.189	0.039	0.091	0.059	1.8	7.0
254	0.30	413	0.194	0.032	0.091	0.072	1.1	5.5

Table 5. Simulated results for varying length and number of thermoelectric pairs.

N	k (W/mK)	$\dot{Q}$ (W)	R (K/W)	R_{eq} (K/W)	R_{hp} (K/W)	R_c (K/W)	P (W)	V (V)
6	-	232	0.344	0.213	0.091	0.040	4.5	11.0
5	10	280	0.286	0.141	0.091	0.054	2.2	7.6
5	25	309	0.259	0.103	0.091	0.065	1.4	6.1
5	50	319	0.251	0.085	0.091	0.075	1.0	5.2
5	75	321	0.249	0.077	0.091	0.081	0.9	4.8
5	100	322	0.249	0.074	0.091	0.084	0.8	4.5
5	200	321	0.249	0.067	0.091	0.091	0.7	4.2
4	10	293	0.273	0.105	0.091	0.077	1.0	5.0
4	25	297	0.269	0.067	0.091	0.111	0.4	3.3
4	35	289	0.277	0.059	0.091	0.127	0.3	2.8
4	50	277	0.289	0.053	0.091	0.145	0.2	2.4

Table 6. Simulated results for varying thermal bridge conductivity and number of thermoelectric modules.

Figure1

Click here to download high resolution image

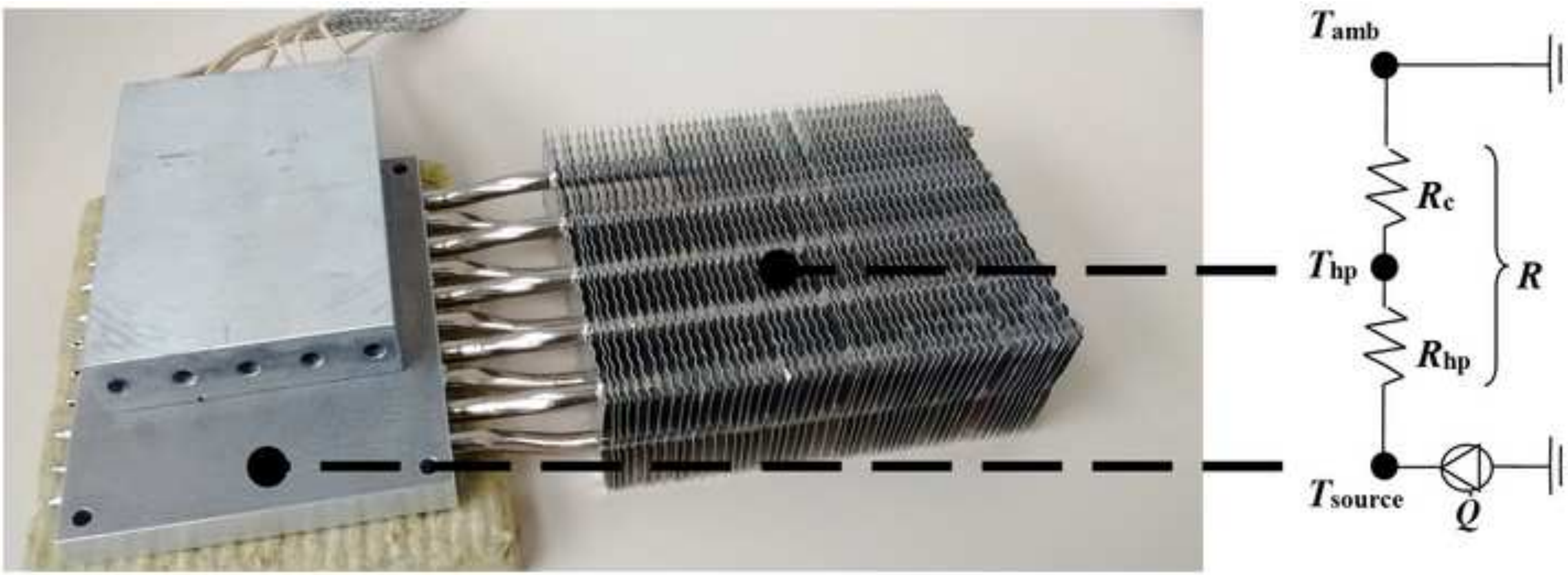

Figure2

Click here to download high resolution image

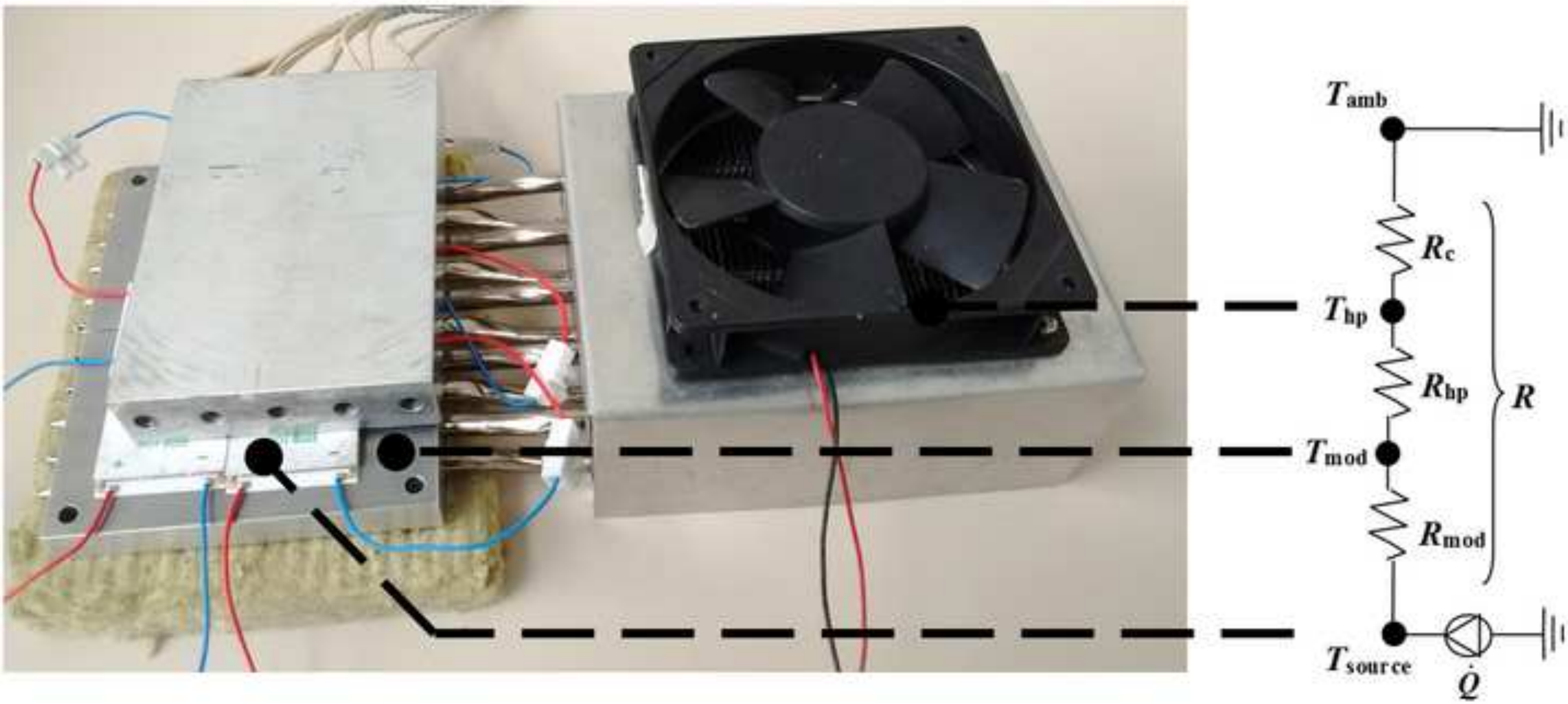

Figure3

Click here to download high resolution image

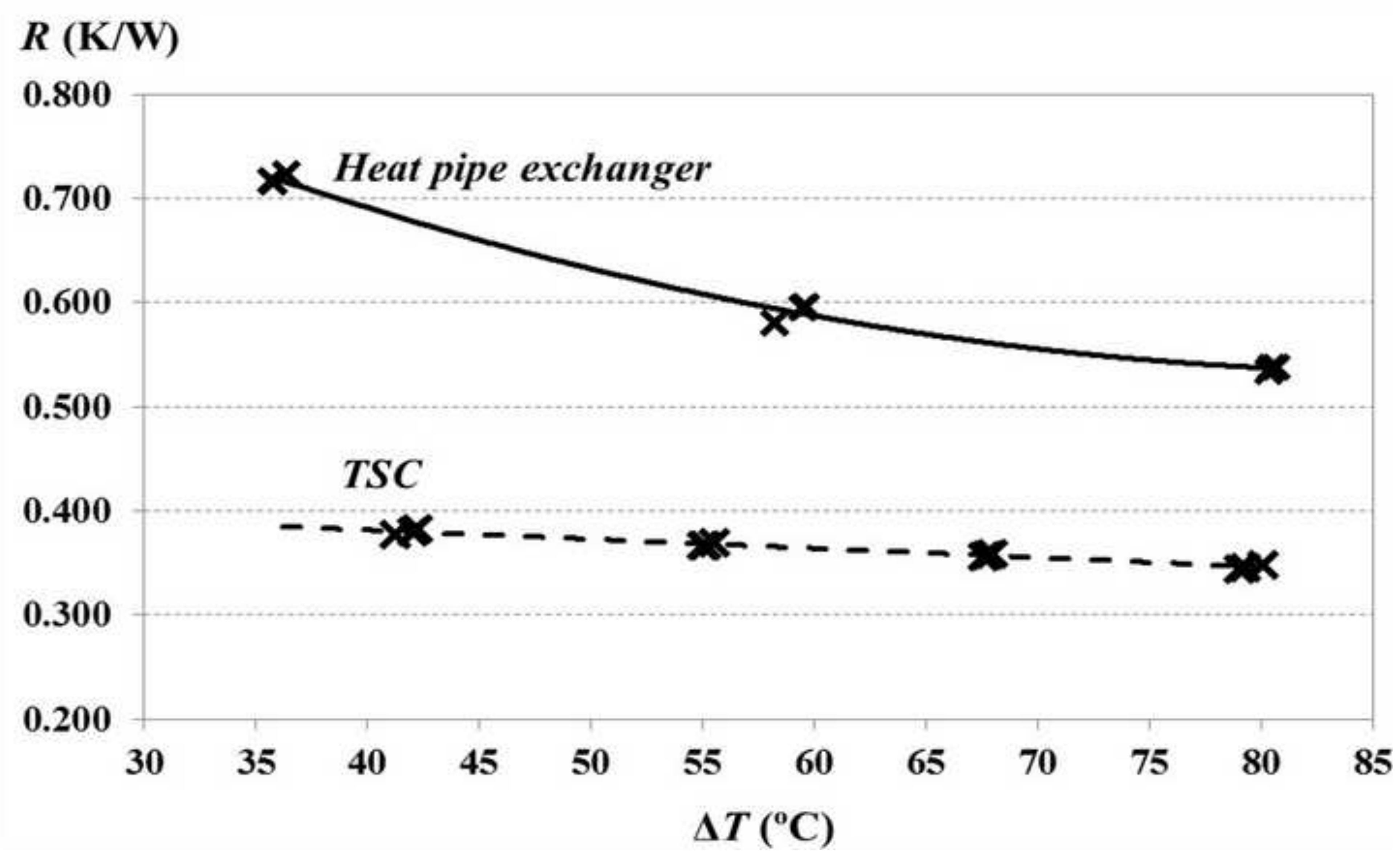

Figure4
Click here to download high resolution image